Zyuzin, Vladimir A.; Zyuzin, Alexander A.

Anisotropic resistivity and superconducting instability in ferroelectric metals

Published in:
Physical Review B

DOI:
10.1103/PhysRevB.106.L121114

Published: 15/09/2022

Document Version
Publisher's PDF, also known as Version of record

Please cite the original version:
Zyuzin, V. A., & Zyuzin, A. A. (2022). Anisotropic resistivity and superconducting instability in ferroelectric metals. *Physical Review B*, *106*(12), 1-6. Article L121114. https://doi.org/10.1103/PhysRevB.106.L121114

Letter

Anisotropic resistivity and superconducting instability in ferroelectric metals

Vladimir A. Zyuzin [1] and Alexander A. Zyuzin [2]
[1] *L. D. Landau Institute for Theoretical Physics, Semenova 1-a, 142432 Chernogolovka, Russia*
[2] *Department of Applied Physics, QTF Centre of Excellence, Aalto University, FI-00076 AALTO, Finland*

(Received 1 March 2022; accepted 13 September 2022; published 26 September 2022)

We propose a theoretical model of a ferroelectric metal where spontaneous electric polarization coexists with the conducting electrons. In our model we adopt a scenario when conducting electrons interact with two soft transverse optical phonons, generalize it to the case when there is a spontaneous ferroelectric polarization in the system, and show that a linear coupling to the phonons emerges as a result. We find that this coupling results in anisotropic electric transport which has a transverse to the current voltage drop. Importantly, the obtained transverse component of the resistivity has distinct linear dependence with temperature. Moreover, we show that the coupling enhances superconducting transition temperature of the ferroelectric metal. We argue that our results help to explain recent experiments on ferroelectric strontium titanate as well as provide new experimental signatures to look for.

DOI: 10.1103/PhysRevB.106.L121114

Introduction. The strontium titanate-based (STO) compound has a rich phase diagram upon chemical doping and temperature variation, which includes seemingly self-exclusive ferroelectric and superconducting states, see, for a review, Refs. [1–3]. To begin with, we note that the pristine $SrTiO_3$ is a wide-band-gap quantum paraelectric insulator. It can be tuned into a ferroelectric state by partial substitution of Sr ions with Ca, Ba, or Pb [4–6], isotope substitution of oxygen [7], and applying stress [8]. The structural formation is associated with the soft transverse optical (TO) lattice vibration. The gap in the dispersion of this phonon mode vanishes at the transition [1,2].

On the other hand, STO becomes semiconducting (or metallic) with partial substitution of Sr with Nb, La, or with oxygen reduction, see, for details, Refs. [1–3]. The charge transport measurements show the square temperature dependence of resistivity within an unusually wide region of material parameters [2,9]. Another remarkable property of the material is the existence of the superconductivity despite of the rather low electron density. Studies of superconductivity in this material have a very long history, [1–3], dating back to experimental work [10]. However, the mechanism of Cooper pairing in STO is still currently under debate. First of all, the superconducting transition temperature mediated by acoustic phonons in STO was estimated to be negligibly small [11], thus, ruling out conventional phonon pairing mechanism. Moreover, the superconductivity in this system emerges in a situation when Fermi energy is an order of magnitude smaller than the Debye frequency. Furthermore, the proximity of the system to a ferroelectric quantum critical point suggests that soft TO phonons might be important.

A possible solution to the problem of superconductivity in STO was proposed a long time ago by Ngai, who introduced a model of superconducting instability based on electron coupling tuned by a pair of TO phonons [12]. In paraelectric STO the electron scattering by transverse phonons is proportional to the second power in lattice displacement amplitude. Below we will be referring to this mechanism as the two-phonon. The two-phonon mechanism is distinct from the electron scattering by acoustic phonons, which is described by the gradient of lattice displacement. Later Epifanov *et al.* studied the T^2 dependence of conductivity due to the two-phonon mechanism near ferroelectric phase transition [13,14].

Recent observation of the enhancement of superconducting transition temperature in STO upon oxygen isotope substitution, which brings the system closer to the ferroelectric transition, has reinvigorated this subject [15]. Proximity to a ferroelectric instability strongly suggests that the soft TO phonons play an influential role. Thus, the model of two-phonon scattering was brought forward to revisit the temperature dependence of charge transport [16,17] and study the effect of oxygen isotope substitution on superconducting transition temperature [18–20].

The story is far from being complete. Recently, the signatures of ferroelectric instability has been observed in *n*-doped $Sr_{1-x}Ca_xTiO_{3-\delta}$, [21–24]. It was found that superconductivity and ferroelectricity may coexist in this material [21,23,24]. The resistivity showed anomalous temperature dependence, suggesting the emergence of an additional scattering channel [22–24]. The coexistence of metallic and ferroelectric phases might be understood within the dipole model. The ferroelectric instability is based on the interplay between the long-range dipole-dipole interaction and the short-range repulsion between ions. The former favors ferroelectric structure formation with the emergence of electric dipole moment per unit cell, and the latter supports the paraelectric phase, please see Ref. [25], and for a review, see Ref. [26]. In metals, itinerant electrons screen dipole-dipole interaction and, thus, eliminate ferroelectricity. However, supported by the experiments [21–24], ferroelectricity may survive in weakly doped

semiconductors presumably due to the long Thomas-Fermi screening length or local-bonding contributions [27].

Motivated by these experiments, [21–24], we propose and study a model of electron scattering by one TO phonon in the presence of spontaneous ferroelectric polarization (the one-phonon mechanism). The model is a generalization of the two-phonon mechanism [12] to the ferroelectricity, and adds up with two-phonon mechanism [12–14]. We show that below the structural transition, the decrease in temperature enhances electric resistivity due to the onset of ferroelectric polarization. At lower temperatures, we predict linear in temperature suppression of resistivity. We also calculate the contribution of one-phonon scattering processes to the superconducting transition temperature. We argue that our mechanism might dominate over the two-phonon mediated pairing deep in the ferroelectric phase.

Model. We start with introducing a model of a ferroelectric metal (polar metal), which consists of electrons interacting with TO phonons. The TO phonons are responsible for the ferroelectricity in the system, whereas the electrons are responsible for the electric conduction. The electrons are described by the Hamiltonian,

$$H_{\rm e} = \int_{\mathbf{r}} \psi^\dagger(x)\left(-\frac{\partial_{\mathbf{r}}^2}{2m} - \mu\right)\psi(x), \tag{1}$$

where $\psi^\dagger(x), \psi(x)$ are the electron creation and annihilation operators, μ is the chemical potential, m is the mass of electrons, $x = (\mathbf{r}, t)$ is a general coordinate, and $\int_{\mathbf{r}}(\cdots) \equiv \int d\mathbf{r}(\cdots)$. The Hamiltonian of two degenerates denoted by $a = 1, 2$ branches of TO phonons is

$$H_{\rm ph}^{(a)} = \sum_{\mathbf{q}} \omega_{\mathbf{q}}\left(b_{a;\mathbf{q}}^\dagger b_{a;\mathbf{q}} + \frac{1}{2}\right), \tag{2}$$

where $\omega_{\mathbf{q}} = \sqrt{\omega_{\rm TO}^2 + s^2 q^2}$ is the spectrum with s being the speed of sound and $\omega_{\rm TO}$ being the TO phonon gap. Polarization vector $\mathbf{P}(x)$ describing the TO phonons is

$$\mathbf{P}(x) = \sum_{a;\mathbf{q}} \frac{\mathbf{e}_{a;\mathbf{q}}}{\sqrt{V}} A_{\mathbf{q}}[b_{a;\mathbf{q}}(t)e^{i\mathbf{qr}} + b_{a;\mathbf{q}}^\dagger(t)e^{-i\mathbf{qr}}], \tag{3}$$

where V is the volume of the material, $\mathbf{e}_{a;\mathbf{q}}$ is the unit vector in the direction of polarization of $a = 1, 2$ branches of TO phonons with wave-vector $\mathbf{q}$, and $b_{a;\mathbf{q}}^\dagger$, $b_{a;\mathbf{q}}$ are the bosonic creation and annihilation operators. We consider $A_{\mathbf{q}}^2 = \Omega_0^2/(4\pi\omega_{\mathbf{q}})$, where Ω_0 is a material-dependent coefficient determined via Lyddane-Sachs-Teller relation for the static dielectric function $\epsilon_0(\mathbf{q}) = \Omega_0^2/\omega_{\mathbf{q}}^2$ [16]. The identity unit vectors satisfy is

$$\sum_{a=1,2} e_{a;\mathbf{q},\alpha} e_{a;\mathbf{q},\beta} = \delta_{\alpha\beta} - \frac{q_\alpha q_\beta}{q^2}, \tag{4}$$

where $\alpha, \beta = x, y, z$. We assume that $\omega_{\rm TO}$ vanishes at temperature $T_{\rm FE}$ (ferroelectric - paraelectric transition temperature), and the system becomes ferroelectric below this temperature forming spatially homogeneous spontaneous electric polarization $\langle \mathbf{P}(x)\rangle = \mathbf{P}_0$. For temperatures $T < T_{\rm FE}$ the phonon gap is $\omega_{\rm TO} \propto |\mathbf{P}_0|$.

We assume that in the paraelectric state electrons interact with two TO phonons, [12–14]. Namely, it is impossible for electrons to interact with one TO phonon via $\propto [\mathrm{div}\cdot \mathbf{P}(x)]\psi^\dagger(x)\psi(x)$ term (of the Frohlich type), however, it is possible for electrons to interact with two TO phonons via $\propto \mathbf{P}(x)\cdot\mathbf{P}(x)\psi^\dagger(x)\psi(x)$ term. In what follows, we generalize the two-phonon mechanism to the ferroelectric case when $\langle \mathbf{P}(x)\rangle = \mathbf{P}_0$ in the system. We then write for the interaction between electrons and the TO phonons,

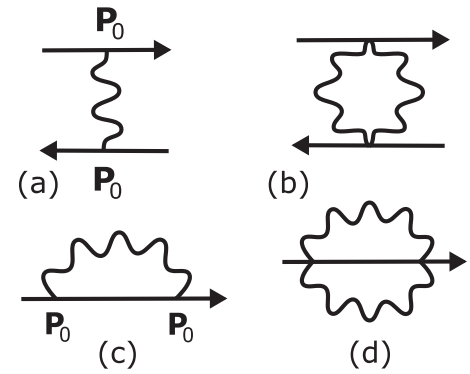

FIG. 1. Feynman diagrams for (a) and (b) the effective electron interaction and (c) and (d) self-energy. Here the wavy line is the phonon Green's function. Object $\mathbf{P}_0$ in (a) and (c) denotes the one-phonon contribution to the interaction in case of ferroelectric order. (b) and (d) describe two-phonon interaction.

$$H_{\text{e-ph}} = g\int_{\mathbf{r}} [\mathbf{P}_0 + \mathbf{P}(x)]^2 \psi^\dagger(x)\psi(x), \tag{5}$$

where g is the electron-phonon interaction constant. We will be using $\hbar = k_{\rm B} = 1$ units throughout the paper.

We note in passing that we do not consider Coulomb repulsion between the electrons and the focus on the electron-phonon interaction only. The reason for that is the large dielectric constant. Moreover, we assume that the electrons do not screen finite electric polarization $\mathbf{P}_0$.

Effective electron interaction. Here we discuss corrections to electron quantum lifetime and conductivity due to the electron-phonon interaction. We choose to work in Keldysh formalism as it conveniently describes fluctuations of the system about its equilibrium at finite temperatures, please see the Supplemental Material (SM) [28].

In order to obtain effective electron interaction, as usual, we integrate out the phonons. To second order in electron-phonon interaction we obtain two processes shown in Figs. 1(a) and 1(b). Processes Fig. 1(b) describe interaction of electrons with two TO phonons [due to $\propto \mathbf{P}^2(x)$ in Eq. (5)], whereas those in Fig. 1(a) describe the interaction of electrons with one TO phonon [due to $\propto \mathbf{P}_0\cdot\mathbf{P}(x)$ in Eq. (5)] given that there is a spontaneous electric polarization $\mathbf{P}_0$ in the system. The processes in Fig. 1(b) were studied in Refs. [12–14,16–20], and we refer to these works for details, the processes in Fig. 1(a) are new and are the subject of the following analysis. The effective electron interaction due to these processes [wavy line in Figs. 1(a) and 1(c)] is

$$V_1^{\rm R/A}(\mathbf{q};\omega) = (2gP_0A_{\mathbf{q}})^2 \sin^2(\phi_{\mathbf{qP}_0}) D^{\rm R/A}(\mathbf{q};\omega), \tag{6}$$

where $D^{R/A}(\mathbf{q};\omega) = 2\omega_{\mathbf{q}}/[(\omega \pm i0)^2 - \omega_{\mathbf{q}}^2]$ is the TO phonon (retarded/advanced) Green's function. We have defined an angle between $\mathbf{q}$ and $\mathbf{P}_0$ as $\cos(\phi_{\mathbf{qP}_0}) \equiv (\mathbf{q}\cdot\mathbf{P}_0)/(qP_0)$.

With all the details given in the SM [28] we here present essential results and experimental predictions of the model.

Self-energy and resistivity. The experiments, see, for a review, Refs. [1,2] show that the resistivity of metallic STO is proportional to T^2 at low temperatures. In a typical Fermi liquid, such temperature dependence originates from the electron-electron Coulomb interaction. However, in metallic STO, due to a large dielectric constant, Coulomb interaction is expected to be weak. In Refs. [13,14,16–18] it was theoretically suggested that the T^2 contribution to the resistivity due to the two-phonon mechanism can be significant. Namely, the self-energy Fig. 1(d) due to the electron-phonon processes which are depicted in Fig. 1(b) results in the decay-rate proportional to the T^2, which is independent of the electronic density of states [16].

In another set of experiments Refs. [21–23] it was observed that substitution of Sr atoms with Ca, i.e., by creating $Sr_{1-x}Ca_xTiO_3$ compound, results in the ferroelectric transition of the material. Moreover, it was shown that the ferroelectric order survives when the $Sr_{1-x}Ca_xTiO_3$ is made metallic by doping it. Furthermore, the experiments clearly observe a new boson mode the conducting electrons scatter by in the ferroelectric phase, which results in the nonmonotoneous temperature dependence of the resistivity in the vicinity of the ferroelectric transition [21–23].

Let us analyze how the electron scattering on one-phonon interaction derived in Eq. (6) affects the resistivity of the system. Taking the imaginary part of the electron-self energy Fig. 1(c) and setting frequency to zero, we find the electron decay rate due to scattering via one-phonon mechanism, $\tau_{1\mathbf{k}}^{-1}$. Setting momentum of the electron $k = k_F \equiv \sqrt{2m\mu}$, we obtain

$$\frac{1}{\tau_{1\mathbf{k}}} = 2\left[1+\cos^2(\phi_{\mathbf{kP}_0})\right]\left(2\pi g\frac{\Omega_0 P_0}{T_{BG}}\right)^2 \nu \times T\,\ln\left|\tanh\left(\frac{\sqrt{T_{BG}^2+\omega_{TO}^2}}{2T}\right)\coth\left(\frac{\omega_{TO}}{2T}\right)\right|, \quad (7)$$

where $\nu = mk_F/2\pi^2$ is the density of electron states per spin and $T_{BG} = 2sk_F$ is the Bloch-Gruneisen temperature. Let us separate the isotropic part from the angle-dependent one by a redefinition of $\tau_{1\mathbf{k}}^{-1} \equiv \tau_1^{-1}[1+\cos^2(\phi_{\mathbf{kP}_0})]$.

The temperature dependence of the isotropic part of the decay rate is shown in Fig. 1(a). At the ferroelectric transition $P_0 \to 0$ in the prefactor of Eq. (7) taking care of the logarithm, which formally diverges due to $\omega_{TO} \to 0$ at the transition. Hence, right at the transition the decay rate vanishes as shown in Fig. 1(a). Slightly below the ferroelectric transition $T_{FE} \gtrsim T$, the decay rate increases with the decrease in temperature as shown in Fig. 2. We may assume P_0 and ω_{TO} to be temperature independent far from the transition. In this case, at $T_{FE} > T \gtrsim T_{BG}, \omega_{TO}$, the decay rate scales linearly with temperature, and for the region $T_{FE}, T_{BG} > T > \omega_{TO}$, we find $\tau_1^{-1} \propto T\,\ln|2T/\omega_{TO}|$. As another example, let us note that $\tau_1 \propto k_F$ at $T > T_{BG}$. It is drastically different from

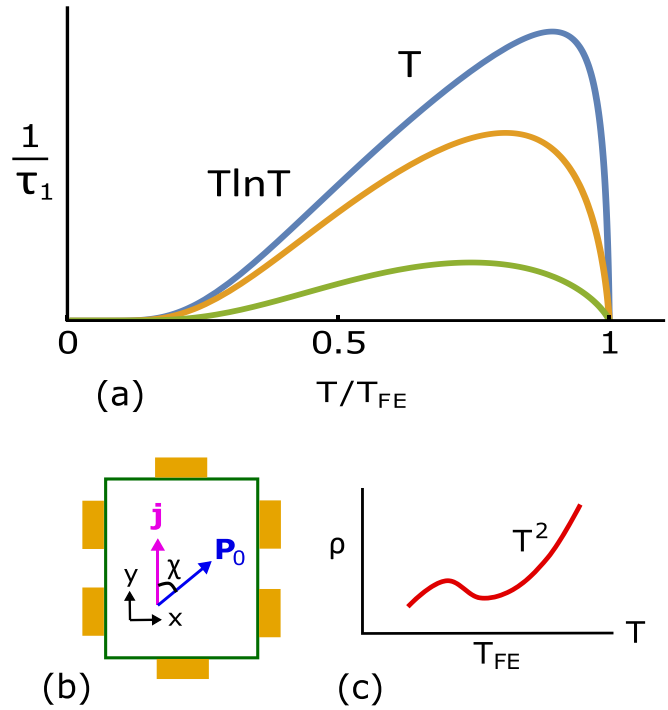

FIG. 2. (a) Temperature dependence of the decay rate due to electron scattering by one TO phonon. Assuming temperature dependence in $P_0^2(T) \propto \omega_{TO}^2(T) = \omega_{TO}^2(0)(1 - T/T_{FE})$, the curves are plotted for $T_{BG}/\omega_{TO}(0) = \{0.2, 0.5, 1.5\}$. The amplitude decreases with the increase in $T_{BG}/\omega_{TO}(0)$. (b) Schematics of the Hall bar to measure the electric transport anisotropy given in Eq. (8). With the direction of the electric polarization being on the x-y plane, the current is passed at some angle χ with respect to the polarization, for example, in the y direction. (c) Schematics of the temperature dependence of the longitudinal resistivity given in Eq. (8). For $T > T_{FE}$ the resistivity is expected to be $\propto T^2$ due to two-phonon mechanism Refs. [13,14,16,17]. Below T_{FE} the one-phonon mechanism Eq. (7) depicted in (a) sets in, in addition to two-phonon $\propto T^2$, resulting in an increase in the resistivity.

the two-phonon process, which is independent of k_F at these temperatures [16]. It is also instructive to compare the obtained decay rate with the one due to electron scattering on acoustic longitudinal phonons (obtained from the Frohlich-type interaction). There, the decay rate is $\propto \nu T/T_{BG}^2$ at high temperatures $T \gg T_{BG}$, whereas $\propto \nu T^3/T_{BG}^2$ at low temperatures $T \ll T_{BG}$ [29,30].

Let us calculate the electric current in the system. In the SM [28], we construct the kinetic equation with the collision integral defined by the impurity, one- and two-phonon scattering processes. The kinetic equation is solved to give the electric current,

$$\mathbf{j} = \sigma\left(1-\frac{\tau}{5\tau_1}\right)\mathbf{E} - \sigma\frac{2\tau}{5\tau_1}(\mathbf{E}\cdot\mathbf{P}_0)\mathbf{P}_0\frac{1}{P_0^2}, \quad (8)$$

in which $\sigma = e^2\nu D$ is the conductivity, where $D = v_F^2\tau/3$ is the diffusion coefficient, and $\tau^{-1} = \tau_{imp}^{-1} + \tau_1^{-1} + \tau_2^{-1}$ is the total decay rate due to the isotropic impurity, one- and two-phonon scattering processes (in general, the decay rate due to the electron-electron Coulomb interaction should also be included).

Obtained anisotropy of the electric current [the second term in Eq. (8)] results in the transverse responses. For example, in Fig. 2(b) we schematically show the Hall-bar setup where the electric current is passed in the y direction at some angle χ to the electric polarization, which is on the x-y plane. The voltage drop in the direction perpendicular to the current is measured either in opposite or along diagonal gates to study the angle dependence, $\propto \cos(\chi)\sin(\chi)$, of the transverse part of Eq. (8). Most importantly, as can be deduced from Eq. (8), only the anisotropic part of the resistivity depends on temperature as shown in Fig. 2(a).

The longitudinal part of the resistivity in the ferroelectric phase is more complicated as the two-phonon mechanism (also impurity scattering and others) contributes to it as well. In Fig. 2(c) we schematically plot the temperature dependence of the longitudinal part of the resistivity Eq. (8). There, for $T > T_{\rm FE}$ the resistivity is expected to be $\propto T^2$ due to the two-phonon mechanism as predicted in Refs. [13,14,16,17]. Below $T_{\rm FE}$ the one-phonon mechanism Eq. (7) sets in resulting in an increase of the resistivity with a characteristic dip at $T_{\rm FE}$. The two-phonon mechanism exists in the ferroelectric phase as well because $\omega_{\rm TO} \to 0$ at the transition, allowing for the $\propto T^2$ results of Refs. [13,14,16,17] to be applicable. We argue that this picture explains experimental results of Refs. [21–23].

We conclude that by subtracting from the longitudinal resistivity its temperature-squared part of the fit in the ferroelectric phase, one should explicitly obtain a one-phonon contribution with a characteristic temperature dependence shown in Fig. 2(a). In addition, the same temperature dependence, shown in Fig. 2(a), is expected in the measured transverse voltage.

Superconducting transition temperature. Let us now proceed with the calculation of correction of one-phonon process to the Cooper pairing in ferroelectric metal. To qualitatively estimate the superconducting transition temperature, we adopt the approach of Refs. [31,32]. The pole in the fermion scattering amplitude in the Cooper channel determines the superconducting transition temperature. The equation for the respective vertex part is given by

$$\Gamma(\mathbf{q}) = V(\mathbf{q}) - \int_{\mathbf{p}} V(\mathbf{q}-\mathbf{p}) \frac{\tanh\left(\frac{\xi_{\mathbf{p}}}{2T}\right)}{2\xi_{\mathbf{p}}} \Gamma(\mathbf{p}). \tag{9}$$

where $\xi_{\mathbf{p}} = \mathbf{p}^2/2m - \mu$, $V(\mathbf{q}) = V_1(\mathbf{q}) + V_2(\mathbf{q})$ is the electron-electron attraction potential to be specified for one and two TO phonon coupling mechanisms, $V_1(\mathbf{q})$ and $V_2(\mathbf{q})$, respectively, in what follows.

Let us first revisit the two-phonon mechanism of superconductivity in paraelectric metal [12,19,20]. At $T_{\rm BG}, \omega_{\rm TO} > T$, estimating $\coth(\omega_{\mathbf{k}}/2T) \approx 1$, we obtain

$$V_2(\mathbf{q}) = -\left(\frac{g\Omega_0^2}{2\pi}\right)^2 \int_{\mathbf{k}} \left\{1 + \frac{[\mathbf{k}\cdot(\mathbf{k}+\mathbf{q})]^2}{\mathbf{k}^2|\mathbf{k}+\mathbf{q}|^2}\right\} \times \frac{1}{\omega_{\mathbf{k}}\omega_{\mathbf{k}+\mathbf{q}}} \frac{1}{\omega_{\mathbf{k}} + \omega_{\mathbf{k}+\mathbf{q}}}. \tag{10}$$

The first factor under the integral originates from the transverse polarization of phonons, whereas the terms on the second line originate from the dispersion dependence of the phonon Green's function. To estimate the transition temperature, we consider (10) in the long-wave limit. Setting $V_2(0)$, we reproduce previous result [19,20],

$$T_c \propto \mu e^{-1/\lambda_2 \nu},$$
$$\lambda_2 = \left(\frac{g\Omega_0^2}{2\pi}\right)^2 \frac{1}{2s^3} \ln\left[\frac{sq_0}{\max(T_{\rm BG}, \omega_{\rm TO})}\right],$$

where q_0 is the large momentum cutoff which is determined by the lattice spacing. It was noted that as the paraelectric system is tuned closer to the ferroelectric instability, the softening of TO phonon gap might enhance the superconducting transition temperature [19,20]. We also note that although due to $\lambda_2 \nu \propto T_{\rm BG} \ln[sq_0/T_{\rm BG}]$, the domelike shape dependence of the superconducting transition temperature on the electron density is expected [20], it is rather beyond the assumed approximations of the theory [19].

We argue that in the ferroelectric metal one-phonon coupling processes will be taken into account as well. The respective interaction term is given by the static part of Eq. (6), $V_1(\mathbf{q}) = -\frac{1}{\pi\omega_{\mathbf{q}}^2}(g\Omega_0 P_0)^2 \sin^2\phi_{\mathbf{q}\mathbf{P}_0}$.

We seek for the transition temperature to s-wave superconducting state. Substituting $V_1(\mathbf{q})$ into Eq. (9) and integrating the resulting equation over the directions of momentum $\mathbf{q}$, in the long-wave limit we obtain

$$T_c \propto \mu \exp\left\{-\frac{1}{(\lambda_1+\lambda_2)\nu}\right\},$$
$$\lambda_1 = \frac{2}{3\pi}\left(\frac{g\Omega_0 P_0}{T_{\rm BG}}\right)^2 \ln\left(\frac{\omega_{\rm TO}^2 + T_{\rm BG}^2}{\omega_{\rm TO}^2}\right). \tag{11}$$

Here we assumed $\omega_{\rm TO} > \frac{s}{v_F}T$. As the system is tuned deep into the ferroelectric state, the phonon gap $\omega_{\rm TO}$ increases and, hence, the two-phonon contribution to the interaction potential decreases logarithmically in accordance with (11). We note that just the two-phonon mechanism gives roughly the same T_c in the paraelectric and ferroelectric versions of the metal (we keep in mind STO [21–24]). This is because $\omega_{\rm TO}$ in the ferroelectric phase of ferroelectric metal increases and can become of the same value as that of the paraelectric metal. On the other hand, the one-phonon mechanism in the ferroelectric phase of the metal adds up to the two-phonon's. The one-phonon mechanism might even be dominant at the superconducting transition temperature at $\omega_{\rm TO} \gg T_{\rm BG}$ provided $P_0/\omega_{\rm TO} \gtrsim (\Omega_0/4\pi s^{3/2})\sqrt{\ln|sq_0/\omega_{\rm TO}|}$. This is consistent with the experiments [21–24] which observe enhancement of T_c inside the ferroelectric phase of the ferroelectric STO as compared to the paraelectric STO.

It is instructive to comment on the density of states dependence of the one-phonon contribution to the transition temperature, noting $\lambda_1\nu \propto T_{\rm BG}^{-1}\ln(1 + T_{\rm BG}^2/\omega_{\rm TO}^2)$. At $\omega_{\rm TO} > T_{\rm BG}$, the exponent in (11) follows the usual BCS dependence on the density of states. However, at $T_{\rm BG} > \omega_{\rm TO}$, with the logarithmic accuracy the interaction constant is inversely proportional to the Bloch-Gruneisen temperature squared, hence, $\lambda_1\nu \propto \nu/T_{\rm BG}^2 \propto m/k_F$. Surprisingly, in this case the decrease of the doping might enhance one-phonon contribution and increase T_c. Based on our findings, the superconducting transition temperature might have domelike shape as a function of carrier concentration in the ferroelectric phase due to the one-phonon contribution.

We note in passing that by approximating angular dependence of one-phonon coupling Eq. (6) by its average (see also Ref. [28]), we have provided arguments for the isotropic superconductivity in the ferroelectric phase. In general, the superconductivity in ferroelectric phase will be anisotropic. Moreover, ferroelectric phase will contain domains with different directions of the electric polarization, which might influence the superconducting temperature [33]. Both questions are left for future research.

Conclusions. To conclude, we showed that a new mechanism of electron interaction with one TO-phonon emerges in the ferroelectric phase of the metal, compared to a well-known [12–14,16–20] two-phonon mechanism in the paraelectric phase. We calculated the temperature dependence of resistivity and predicted anisotropic electric current response as one of the smoking gun signatures of the ferroelectric polarization onset. We also analyzed the superconducting transition temperature in the ferroelectric phase. We think that our results for the temperature dependence of the resistivity in the vicinity of the ferroelectric transition given in Eqs. (7) and (8) as well as for the increase in the superconducting transition temperature given in Eq. (11) qualitatively agree with the experimentally observed ones in $Sr_{1-x}Ca_xTiO_3$ systems [21–24]. In particular, the one-phonon scattering mechanism explains the experimentally observed dip in the resistivity at the ferroelectric transition temperature, and the enhancement of the superconducting transition temperature in the ferroelectric STO.

Acknowledgments. We thank the Pirinem School of Theoretical Physics where all work was initiated for the warm hospitality. We thank A. T. Burkov and A. Y. Zyuzin for helpful discussions. V.A.Z. thanks A. Kumar and D. L. Maslov for hospitality during his stay at the UF. V.A.Z. is supported by the Russian Foundation for Basic Research (Grant No. 20-52-12 013), Deutsche Forschungsgemeinschaft (Grant No. EV 30/14-1) cooperation, and by the Foundation for the Advancement of Theoretical Physics and Mathematics BASIS. A.A.Z. was supported by the Academy of Finland (Project No. 308339) and, in part, by the Academy of Finland Centre of Excellence program (Project No. 336810).

[1] M. N. Gastiasoro, J. Ruhman, and R. M. Fernandes, Superconductivity in dilute $SrTiO_3$: A review, Ann. Phys. (Berlin) **417**, 168107 (2020), eliashberg theory at 60: Strong-coupling superconductivity and beyond.

[2] C. Collignon, X. Lin, C. W. Rischau, B. Fauque, and K. Behnia, Metallicity and superconductivity in doped strontium titanate, Annu. Rev. Condens. Matter Phys. **10**, 25 (2019).

[3] G. Scheerer, M. Boselli, D. Pulmannova, C. W. Rischau, A. Waelchli, S. Gariglio, E. Giannini, D. van der Marel, and J.-M. Triscone, Ferroelectricity, superconductivity, and $SrTiO_3$ - Passions of K. A. Muller, Condens. Matter **5**, 60 (2019).

[4] J. G. Bednorz and K. A. Müller, $Sr_{1-x}Ca_xTiO_3$: An XY Quantum Ferroelectric with Transition to Randomness, Phys. Rev. Lett. **52**, 2289 (1984).

[5] V. V. Lemanov, E. P. Smirnova, P. P. Syrnikov, and E. A. Tarakanov, Phase transitions and glasslike behavior in $Sr_{1-x}Ba_xTiO_3$, Phys. Rev. B **54**, 3151 (1996).

[6] V. V. Lemanov, E. P. Smirnova, and E. A. Tarakanov, Ferroelectric properties of $SrTiO_3$-$PbTiO_3$ solid solutions, Phys. Solid State **39**, 628 (1997).

[7] M. Itoh, R. Wang, Y. Inaguma, T. Yamaguchi, Y.-J. Shan, and T. Nakamura, Ferroelectricity Induced by Oxygen Isotope Exchange in Strontium Titanate Perovskite, Phys. Rev. Lett. **82**, 3540 (1999).

[8] H. Uwe and T. Sakudo, Stress-induced ferroelectricity and soft phonon modes in $SrTiO_3$, Phys. Rev. B **13**, 271 (1976).

[9] K. Behnia, On the origin and the amplitude of T-square resistivity in Fermi liquids, Ann. Phys. (Berlin) **534**, 2100588 (2022).

[10] J. F. Schooley, W. R. Hosler, and M. L. Cohen, Superconductivity in Semiconducting $SrTiO_3$, Phys. Rev. Lett. **12**, 474 (1964).

[11] J. Ruhman and P. A. Lee, Superconductivity at very low density: The case of strontium titanate, Phys. Rev. B **94**, 224515 (2016).

[12] K. L. Ngai, Two-Phonon Deformation Potential and Superconductivity in Degenerate Semiconductors, Phys. Rev. Lett. **32**, 215 (1974).

[13] Y. N. Epifanov, A. P. Levanyuk, and G. M. Levanyuk, Interaction of carriers with TO phonons and electrical conductivity of ferroelectrics, Ferroelectrics **35**, 199 (1981).

[14] Y. N. Epifanov, A. P. Levanyuk, and G. M. Levanyuk, Interaction of carriers with soft ferroelectric mode and temperature dependence of conductivity, Ferroelectrics **43**, 191 (1982).

[15] A. Stucky, G. W. Scheerer, Z. Ren, D. Jaccard, J. M. Poumirol, C. Barreteau, E. Giannini, and D. van der Marel, Isotope effect in superconducting n-doped $SrTiO_3$, Sci. Rep. **6**, 37582 (2016).

[16] A. Kumar, V. I. Yudson, and D. L. Maslov, Quasiparticle and Nonquasiparticle Transport in Doped Quantum Paraelectrics, Phys. Rev. Lett. **126**, 076601 (2021).

[17] K. G. Nazaryan and M. V. Feigel'man, Conductivity and thermoelectric coefficients of doped $SrTiO_3$ at high temperatures, Phys. Rev. B **104**, 115201 (2021).

[18] D. van der Marel, F. Barantani, and C. W. Rischau, Possible mechanism for superconductivity in doped $SrTiO_3$, Phys. Rev. Res. **1**, 013003 (2019).

[19] D. E. Kiselov and M. V. Feigel'man, Theory of superconductivity due to Ngai's mechanism in lightly doped $SrTiO_3$, Phys. Rev. B **104**, L220506 (2021).

[20] P. A. Volkov, P. Chandra, and P. Coleman, Superconductivity from energy fluctuations in dilute quantum critical polar metals, Nat. Commun. **13**, 4599 (2022).

[21] C. W. Rischau, X. Lin, C. P. Grams, D. Finck, S. Harms, J. Engelmayer, T. Lorenz, Y. Gallais, B. Fauquy, J. Hemberger, and K. Behnia, A ferroelectric quantum phase transition inside the superconducting dome of $Sr_{1-x}Ca_xTiO_{3-\delta}$, Nat. Phys. **13**, 643 (2017).

[22] J. Wang, L. Yang, C. W. Rischau, Z. Xu, Z. Ren, T. Lorenz, J. Hemberger, X. Lin, and K. Behnia, Charge transport in a polar metal, npj Quantum Mater. **4**, 61 (2019).

[23] C. W. Rischau, D. Pulmannová, G. W. Scheerer, A. Stucky, E. Giannini, and D. van der Marel, Isotope tuning of the superconducting dome of strontium titanate, Phys. Rev. Res. **4**, 013019 (2022).

[24] Y. Tomioka, N. Shirakawa, and I. H. Inoue, Superconductivity enhanced in the polar metal region of $Sr_{0.95}Ba_{0.05}TiO_3$ and $Sr_{0.985}Ca_{0.015}TiO_3$ revealed by the systematic Nb doping, arXiv:2203.16208.

[25] R. Cohen, Origin of ferroelectricity in perovskite oxides, Nature (London) **358**, 136 (1992).

[26] W. X. Zhou and A. Ariando, Review on ferroelectric/polar metals, Jpn. J. Appl. Phys. **59**, SI0802 (2020).

[27] N. A. Benedek and T. Birol, 'Ferroelectric' metals reexamined: fundamental mechanisms and design considerations for new materials, J. Mater. Chem. C **4**, 4000 (2016).

[28] See Supplemental Material at http://link.aps.org/supplemental/10.1103/PhysRevB.106.L121114 for the details of a ferroelectric model; the derivations of self-energy of electrons due to interaction with TO phonons, the electron-phonon collision integral, and the electric current density, which includes Refs. [34] and [35].

[29] P. B. Allen and R. Silberglitt, Some effects of phonon dynamics on electron lifetime, mass renormalization, and superconducting transition temperature, Phys. Rev. B **9**, 4733 (1974).

[30] A. B. Migdal, Interaction between electrons and lattice vibrations in a normal metal, Zh. Eksp. Teor. Fiz. **34**, 1438 (1958) [Sov. Phys. JETP **7**, 996 (1958)].

[31] L. P. Gor'kov and T. K. Melik-Barkhudarov, Contribution to the theory of superfluidity in an imperfect Fermi gas, Zh. Eksp. Teor. Fiz. **40**, 1452 (1961) [Sov. Phys. JETP **13**, 1018 (1961)].

[32] L. P. Gor'kov, Superconducting transition temperature: Interacting Fermi gas and phonon mechanisms in the nonadiabatic regime, Phys. Rev. B **93**, 054517 (2016).

[33] S. Hameed, D. Pelc, Z. Anderson, A. Klein, R. J. Spieker, B. Yue, L. ans Das, J. Ramberger, M. Lukas, Y. Liu, M. J. Krogstad, R. Osborn, Y. Li, C. Leighton, R. M. Fernandes, and M. Greven, Enhanced superconductivity and ferroelectric quantum criticality in plastically deformed strontium titanate, Nature Mater. **21**, 54 (2022).

[34] A. Kamenev, *Field Theory of Nonequilibrium Systems* (Cambridge University Press, Cambridge, UK, 2012).

[35] A. A. Abrikosov, L. P. Gorkov, and I. E. Dzyaloshinskii, *Methods of Quantum Field Theory in Statistical Physics* (Dover, New York, 1975).